Cell, Vol. 87, 227–239, October 18, 1996, Copyright ©1996 by Cell Press

Mena, a Relative of VASP and Drosophila Enabled, Is Implicated in the Control of Microfilament Dynamics

Frank B. Gertler,* Kirsten Niebuhr,† Matthias Reinhard,‡ Jürgen Wehland,† and Philippe Soriano*

*Division of Molecular Medicine
Fred Hutchinson Cancer Research Center
1124 Columbia Street
Seattle, Washington 98104

†Gesellschaft für Biotechnologische Forschung mbH
38124 Braunschweig
Germany

‡Medizinische Universitätsklinik
97080 Würzburg
Germany

Summary

Drosophila Enabled is required for proper formation of axonal structures and is genetically implicated in signaling pathways mediated by Drosophila Abl. We have identified two murine proteins, Mena and Evl, that are highly related to Enabled as well as VASP (Vasodilator-Stimulated Phosphoprotein). A conserved domain targets Mena to localized proteins containing a specific proline-rich motif. The association of Mena with the surface of the intracellular pathogen Listeria monocytogenes and the G-actin binding protein profilin suggests that this molecule may participate in bacterial movement by facilitating actin polymerization. Expression of neural-enriched isoforms of Mena in fibroblasts induces the formation of abnormal F-actin-rich outgrowths, supporting a role for this protein in microfilament assembly and cell motility.

Introduction

The control of cell morphology and motility requires the coupling of external stimuli to processes that alter the cytoskeletal architecture. The mechanical forces that drive morphological change and migration arise initially from the microfilament-based cytoskeleton (recently reviewed by Lauffenburger and Horwitz, 1996; Mitchison and Cramer, 1996). In particular, formation of cellular structures such as filopodia and lammellipodia requires polymerization and stabilization of F-actin. A large body of evidence links various signal transduction pathways to the formation of cellular outgrowths (reviewed by Zigmond, 1996), but the final integration of these signals with regulation of de novo actin polymerization is a complex process that remains to be elucidated.

The migration of neuronal growth cones is a well-studied paradigm for the actin-driven formation of membrane protrusions (Forscher et al., 1992). Establishment of proper connections in the central nervous system depends on the ability of neuronal growth cones to guide neurites to their final targets. Genetic analyses have been used to probe the relationship between signal transduction pathways and neuronal development. One signaling pathway implicated in the processes of axonal outgrowth and fasciculation is mediated by the Drosophila homolog of the c-Abl tyrosine kinase (Gertler et al., 1989, 1993; Henkemeyer et al., 1990). Simple *Abl* mutant animals survive past metamorphosis. However, *Abl* mutants that are also heterozygous for a mutation in *Disabled* (*Dab*), or one of 4 other loci identified in genetic modifier screens, require Abl tyrosine kinase activity for postpupal viability and proper formation of the embryonic central nervous system (CNS). Animals that are homozygous mutant for both *Abl* and *Dab* make few or no proper axonal connections.

The defects caused by loss of Abl, Dab, or both are ameliorated by mutations in the *Enabled* (*Ena*) gene (Gertler et al., 1990, 1995). *Ena* was the only locus recovered in genetic screens for dose-dependent suppressors of *Abl*- and *Dab*-dependent phenotypes. In the homozygous state, *Ena* mutations cause a recessive lethal phenotype that includes defects in the embryonic CNS. Ena protein colocalizes with Abl and Dab in CNS axons and has a proline-rich core that binds in vitro to the SH3 domains of Abl and Src. Ena is tyrosine phosphorylated in vivo, and the phosphotyrosine content of Ena is reduced ~3-fold in *Abl* mutant pupae, indicating that Ena is phosphorylated by Abl-dependent and independent tyrosine kinases. Abl-mediated phosphorylation of Ena is not absolutely required for axonogenesis as the need for Abl tyrosine kinase activity in this process is exposed only in combination with mutations in sensitizing loci such as *Dab* (Henkemeyer et al., 1990).

We sought to expand our understanding of Ena function through the use of the tools available for cell biological and biochemical studies in mammalian systems and have identified two murine proteins, Mena and Evl, with significant similarity to Ena. These molecules comprise a new family of related sequences that includes the vasodilator-stimulated phosphoprotein (VASP) (Haffner et al., 1995), a protein originally identified in platelets as an abundant in vivo substrate for cyclic nucleotide–dependent kinases (Halbrügge and Walter, 1989). In various cell types, the VASP protein is detectable along filamentous structures, in the peripheral lamellae of spreading or migrating cells, and is particularly concentrated at sites of focal and cell–cell contacts (Reinhard et al., 1992).

Two observations implicate VASP in the regulation of microfilament assembly. First, VASP is a ligand for profilin (Reinhard et al., 1995a), an actin-monomer binding protein that can stimulate the formation of F-actin (Pantaloni and Carlier, 1993; reviewed by Theriot and Mitchison, 1993). Second, VASP is recruited to the surface of the intracellular pathogen Listeria monocytogenes through a direct interaction with the bacterial surface protein ActA (Chakraborty et al., 1995; Pistor et al., 1995). Listeria motility results from the rapid polymerization of F-actin at one pole of the bacterium, a process that requires the bacterial protein ActA and is enhanced by host profilin (reviewed by Pollard, 1995; Theriot, 1995; Lasa and Cossart, 1996). The properties of VASP make it a candidate host factor that can mediate the recruitment of profilin to the surface of Listeria, and thus promote F-actin assembly.

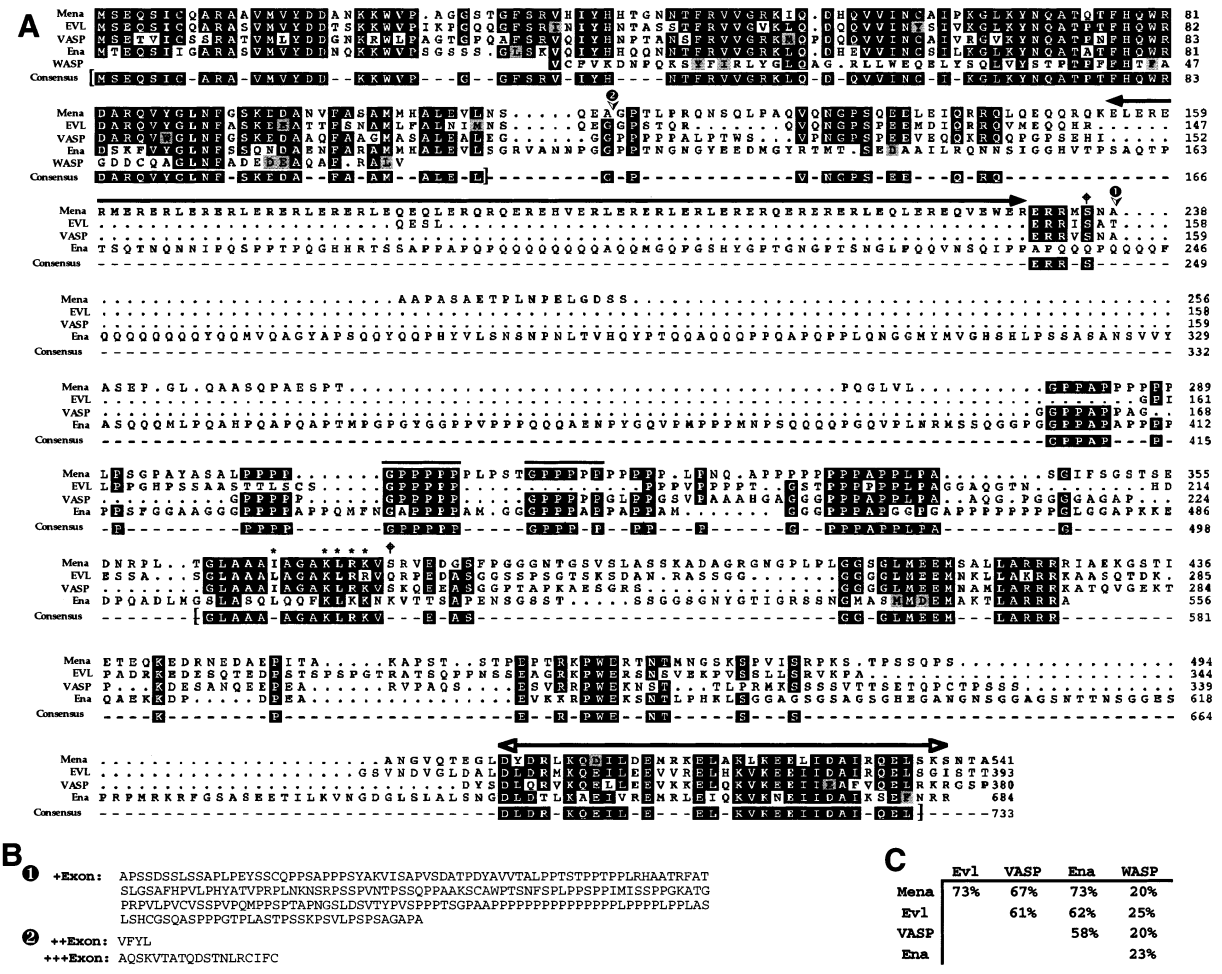

Figure 1. Aligned Sequences of the Ena/VASP Family

(A) Black shading indicates amino acid identity while pale shading indicates a conservative substitution. The deduced amino acid sequence for the 80 kDa form of Mena is shown. Amino acids 72–140 of human WASP are included. The locations of the EVH1 and EVH2 domains, residues 1–133 and 507–733, respectively, are indicated by brackets on the consensus line. The central proline-rich region of Mena is flanked by serine residues (indicated by a circled cross) that align to two of the known cyclic nucleotide kinase-dependent phosphorylation sites in VASP; Evl contains the amino-terminal site only, while Ena lacks both sites. The sequence GPPPPP, implicated in profilin-binding, is present three times in VASP, twice in Mena (indicated by an overline) and once in Evl. The EVH2 domain contains a motif similar to one critical for the binding of G-actin by thymosinβ4 (KLKR; Van Troys et al., 1996; indicated by asterisks), and a conserved charged cluster at the extreme carboxyl terminus. Two potential extended helical structures in Mena are overlined with double arrowheads. The positions of alternately included exons in Mena are indicated by a circled 1 and a circled 2.

(B) Sequences of exons included in neural-specific variants of Mena. The larger exon (+) at position marked by circled 1 is included in all neural Mena isoforms. None or one of two (++, or +++) sequences at position marked by circled 2 are included.

(C) Percent amino acid identity amongst Ena/VASP proteins and WASP in the interval spanning amino acids 36–115 of the alignment as calculated by the Homologies program.

In this report, we present analyses of the biochemical, cell biological, and functional properties of Mena. Mena is shown to be localized to regions of dynamic actin formation within cells. We define a conserved domain of Mena that directs its subcellular distribution by association with proteins containing a specific proline-rich motif and show that Mena is a ligand for profilin. Finally, we demonstrate that some isoforms of Mena are capable of inducing the formation of actin-rich cellular outgrowths. Our results suggest a role for this new protein in the organization of the microfilament-based cytoskeleton and implicate Mena in the regulation of actin-based cell motility.

Results

Similarity and Domain Structure of the Ena/VASP Protein Family

A probe from Drosophila *Ena* was used to isolate murine cDNAs. Analysis of overlapping cDNAs identified an open reading frame predicted to encode a 541 amino acid protein similar to Drosophila Ena, which we termed mammalian Ena (Mena; Figure 1A). The presence of larger proteins immunologically related to Mena in embryonic head extracts (see below and Figure 2) prompted us to screen a mouse brain cDNA library. Using *Mena* as a probe, cDNAs containing combinations

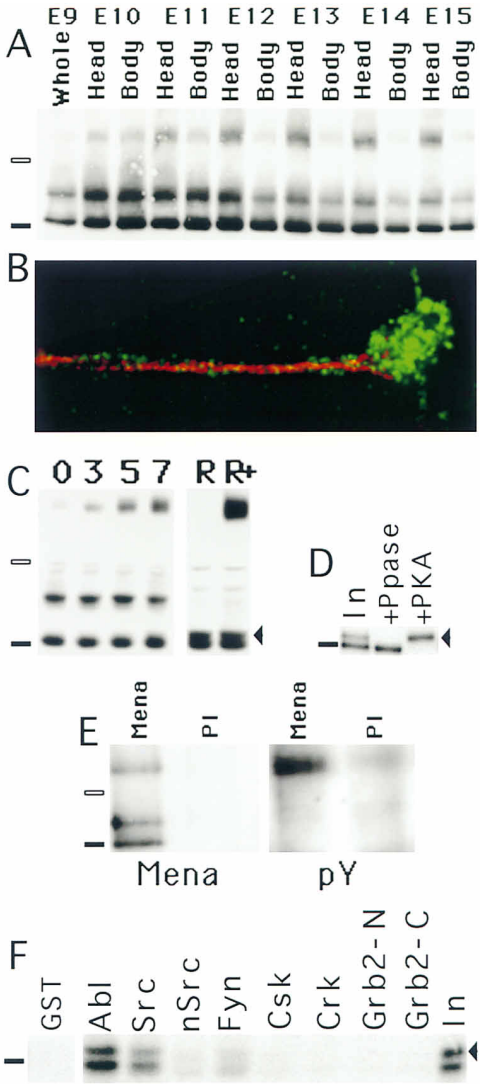

Figure 2. Expression and Phosphorylation of Mena Isoforms

(A) Anti-Mena Western blot analyses of lysates made from E9 embryos, and head and body fractions from E10–E15 embryos. The open and closed bars indicate the positions of the 116 and 80 kDa markers, respectively.

(B) Immunofluorescence of a differentiated P19 cell shows the distribution neurofilament (red) and Mena (green) immunoreactivity. Mena immunoreactivity is also observed along the length of the neurite and in the cell body (not shown).

(C) Anti-Mena Western blot analyses of lysates from P19 cells at 0, 3, 5, and 7 days after treatment with retinoic acid. R and R+ indicate extracts made from RAT2 cells before (R) or after (R+) introduction of a *Mena* cDNA that encodes the neural Mena$^+$ variant. An arrowhead marks the position of a slower migrating form of a doublet derived from the 80 kDa form of Mena.

(D) Phosphatase and kinase treatment of Mena produced in vitro. The input (In), phosphatase-treated (+Ppase), and kinase-treated (+pKA) samples are indicated.

(E) RIPA lysates from E12 embryonic heads were immunoprecipitated using anti-N terminal Mena antibodies or preimmune (PI) sera as indicated. The precipitates were analyzed by Western blotting with anti-C terminal Mena antibodies, or the 4G10 antiphosphotyrosine antibody (pY) as indicated.

(F) SH3 binding of the 80 kDa form of Mena. Immobilized GST or GST-SH3 fusions, as indicated, were incubated in solution with in vitro translated Mena. After washing, retained protein was fractionated by SDS-PAGE and detected by phosphorimager. Ten percent of the amount used in the binding assays was run as loading control (In).

of three alternately included exons (denoted +, ++, and +++) spliced into the original sequence were isolated. All of these larger *Mena* cDNAs contained the + exon, which introduces 246 additional amino acids into the sequence (Figure 1B). Some cDNAs also included either the ++ or the +++ exon as well (Figure 1B).

Database searches identified two more sequences related to Mena, VASP (Haffner et al., 1995) and a human expressed sequence tag (EST). The EST sequence was used to isolate a murine cDNA predicted to encode a 393 amino acid protein that we named Ena-VASP Like (Evl; Figure 1A). Alignment of Mena, Evl, human VASP, and Ena revealed that all contain a central proline-rich core flanked by two highly conserved regions, which we term Ena-VASP homology domains (EVH1 and EVH2; Figure 1A). EVH1 encompasses the WH1 domain (Symons et al., 1996), defined as a block of similarity between the Wiskott-Aldrich syndrome protein (WASP) (Derry et al., 1994) and the VASP and Ena amino termini. A pairwise comparison among the 5 sequences throughout the EVH1 domain revealed that Mena is the vertebrate protein most similar to Ena and VASP, while WASP is the least related (Figure 1C).

In contrast to Ena, VASP, and EVL, Mena contains a striking 5 amino acid repeat region with the consensus sequence LERER, located between the EVH1 domain and the first conserved serine phosphorylation site (Figure 1). The extended helical structure predicted for this repeat may function as a protein-binding interface or to separate the EVH1 domain from the proline-rich core of Mena.

Broadly Distributed and Neural-Enriched Isoforms of Mena

To initiate biochemical and immunocytochemical analyses of Mena, polyclonal antisera were raised against the amino or carboxyl termini of the protein, or a peptide encoding the last 18 amino acids of Mena. Because of the high degree of similarity between Mena and VASP, we tested the Mena sera to ensure that they did not react with VASP. All three anti-Mena sera detected the 541 amino acid form of the Mena protein made in a reticulocyte lysate, while, in Western blot and immunoprecipitation assays, none of the antibodies cross-reacted with purified platelet VASP, or VASP in crude cell lysates (data not shown). The antisera were also tested for cross-reactivity to VASP by immunofluorescent staining of murine macrophages, which contain VASP but no detectable Mena. Staining was not observed with any of the antisera (data not shown), whereas signals were detected in fibroblasts and neurons, both of which express Mena (Figures 2B and 3).

The distribution of Mena during an interval of mouse embryogenesis was determined by Western blot analyses of tissue lysate from dissected embryonic heads and bodies (Figure 2A). Two bands migrating at 80 and 88 kDa were detected in all of the lysates, while a 140 kDa signal was enriched in head fractions and increased

in intensity from E10 to E15, an interval of development during which rapid neurite outgrowth occurs. In adult tissues, the 140 kDa form was found only in brain extracts and not in muscle, lung, kidney, heart, liver, or thymus (data not shown). The 140 kDa band was also enriched during the course of retinoic acid-induced differentiation of P19 embryonic carcinomal stem cells into neurofilament-positive neurons (Figure 2C). In P19 neurons, Mena protein is concentrated in growth cones (Figure 2B); however, isoform-specific antisera will be required to determine the relative distribution of the variants. Similar results in both Western blot and immunofluorescence assays were observed using antisera directed against the amino terminus, carboxyl terminus, or the affinity-purified anti-peptide antibodies; signals were not detected using preimmune sera at the same dilution (data not shown).

The mobility of the 80 and 140 kDa Mena isoforms is slower than predicted by their sequence (60 and 83 kDa, respectively), most likely due to their large proline content. Translation of the *Mena* cDNA in vitro gave rise to proteins that comigrate with the 80 kDa band (Figure 2D). Expression of the neural *Mena*$^{+}$ cDNA in fibroblasts produced a signal at 140 kDa in addition to the endogenous doublet at 80 kDa (Figure 2C). These data indicate that the 80 kDa signal is a broadly expressed form of Mena, while the 140 kDa signal is a Mena isoform enriched in, or specific to, neural cell types and produced by alternative splicing. The 88 kDa signal is immunoreactive with all anti-Mena antibodies tested and likely represents another splice variant or a posttranslationally modified form of Mena. We were unable to recover *Mena* cDNAs that could account for the 88 kDa isoform in screens of four different cDNA libraries or by RT–PCR.

Phosphorylation and SH3-Binding of Mena

Since Ena and VASP are both phosphorylated in vivo, we examined the phosphorylation status of Mena. Mena immunoprecipitates from E12 head lysates contained an anti-phosphotyrosine reactive signal that comigrates with the 140 kDa form (Figure 2E). The 80 and 88 kDa forms contained no detectable phosphotyrosine. In RAT2 cells, Mena migrates as an 80 kDa doublet (Figure 2C) as does Mena protein synthesized in vitro (Figure 2D). To determine if this doublet could be produced by serine-threonine phosphorylation, Mena protein produced in a reticulocyte lysate was immunoprecipitated and incubated with lambda phosphatase. This treatment caused a quantitative conversion of the 80 kDa form of Mena to the faster migrating form of the doublet (Figure 2D), while subsequent treatment of the dephosphorylated sample with protein kinase A shifted the mobility of the protein to the slower migrating form of the doublet (Figure 2D). Thus the slower migrating form of the doublet in RAT2 cells could arise from serine phosphorylation of the 80 kDa form. Therefore, Mena could receive signals from serine-threonine kinase- and, in neurons, tyrosine kinase-mediated-signaling pathways. Since the proline-rich core of Ena can bind to the SH3 domains of Src and Abl (Gertler et al., 1995), we examined whether Mena would associate with GST-SH3 fusion proteins in solution. Mena bound well to the Abl and Src SH3 domains (Figure 2F), but only very weakly to Fyn SH3, and not detectably to neuronal-Src, Grb2, Crk, and Csk SH3 domains or the control GST protein.

Localization of Mena to Focal Adhesions Is Mediated by Its N-terminus

The subcellular distribution of Mena in nonneural cell types was determined by immunofluorescence microscopy (Figures 3 and 4). In RAT2 and PtK_2 cells, Mena localized to focal adhesions and, to a lesser extent, leading edges and stress fibers (Figure 3); similar results were observed using amino- or carboxy-terminal anti-Mena sera. Mena localization in focal contacts was coincident with vinculin, a constituent of focal contacts (Geiger et al., 1980) (Figures 3A and 3A′′). Mena distribution was also compared to that of phosphotyrosine, another marker for focal contacts (Maher et al., 1985). Surprisingly, in most focal contacts, Mena was more concentrated in the proximal portions of the phosphotyrosine domain at the ends of F-actin stress fibers (Figure 3C, see magnified inset). This pattern was observed in 267 out of 305 focal adhesions scored in 6 cells, indicating that, in a large fraction of focal adhesions, tyrosine phosphorylated proteins are more heavily concentrated distally to Mena, vinculin, and perhaps other constituents of focal contacts.

VASP interacts directly with zyxin (Reinhard et al., 1995b), a LIM-domain protein localized in focal adhesions (Sadler et al., 1992) that shares a proline-rich motif with vinculin and ActA (Domann et al., 1992). Since the EVH1 domain is the most highly conserved portion of the sequence, we reasoned that it might mediate an interaction with zyxin or vinculin that recruits Mena to focal adhesions in fibroblasts or related structures in other cell types. An immobilized GST-fusion protein containing amino acids 6–170 of Mena (N-Mena), which encompasses the EVH1 domain, was used to capture proteins from lysates of E12 heads, or human erythrocytic leukemia cells (HEL), which are rich in zyxin. Bound proteins were analyzed by Western blotting (Figure 4A) with antibodies to zyxin, vinculin, or the Ack kinase, which contains a related proline-rich motif (Manser et al., 1993). The N-Mena matrix retained >50% of the total endogenous zyxin, while a much smaller fraction of the vinculin present in the lysates was recovered from the N-Mena column. Ack was not observed among the proteins bound to N-Mena, even though it is readily detectable in the lysates. Direct, specific interactions between N-Mena and zyxin or ActA were demonstrated by ligand overlay assays (Figure 4B). Therefore, Mena can associate directly with ActA, zyxin, and probably vinculin—molecules that all share a related proline-rich motif.

Based on these observations, we speculated that binding of N-Mena to its proline-rich ligands might localize it to focal adhesions. We tested this hypothesis by microinjecting the GST-N-Mena fusion protein into PtK_2 cells to see if N-Mena could direct a heterologous protein to focal contacts. Immunofluorescence of the injected cells with anti-GST antibodies demonstrated that the N-Mena sequences directed the fusion protein to

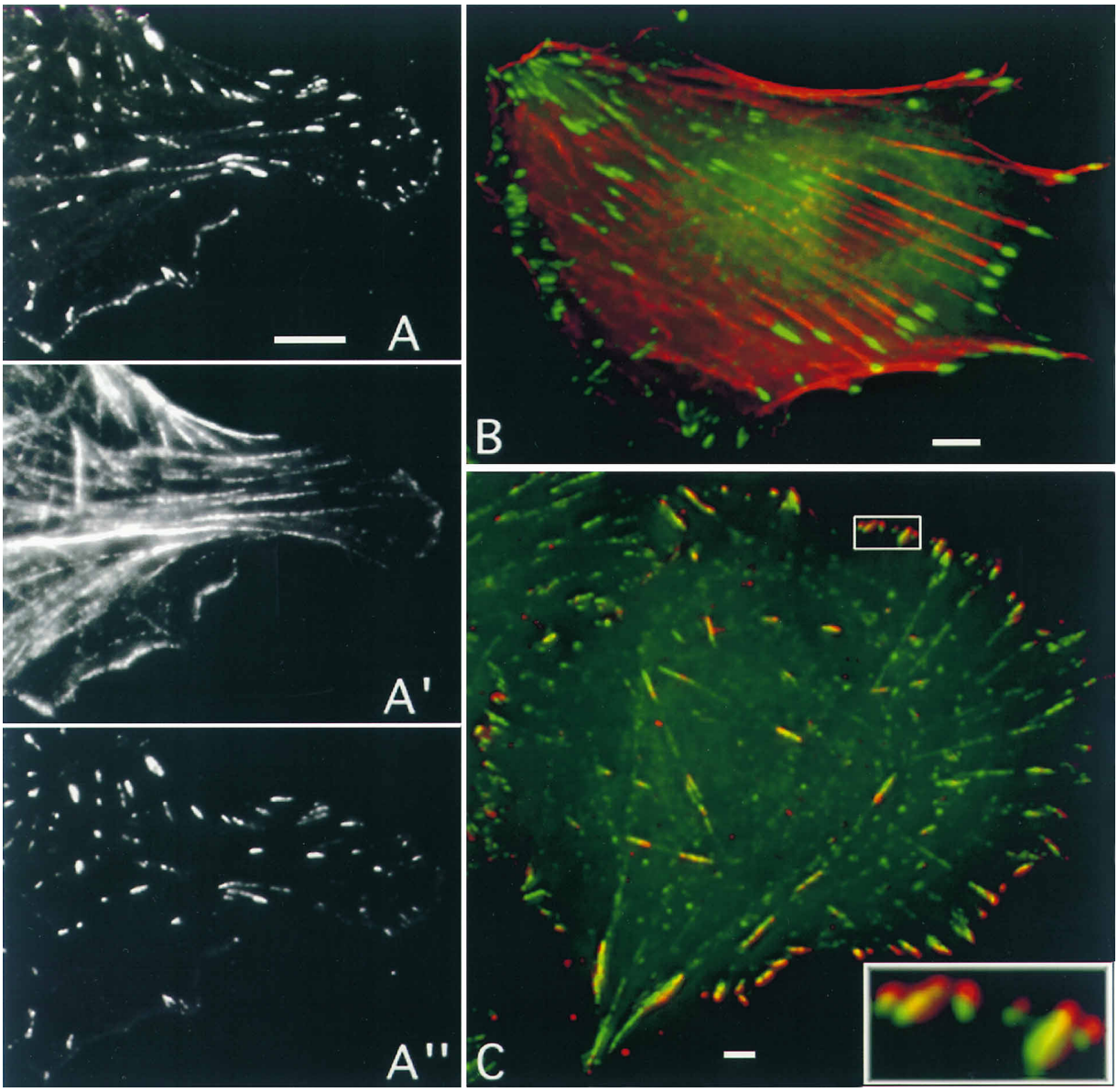

Figure 3. Subcellular Distribution of Mena in RAT2 Cells

(A panels) Immunofluorescence of a lamellipodium shows anti-Mena (A), and anti-vinculin (A′′) immunoreactivity and the distribution of actin stress fibers as indicated by phalloidin labeling (A′).

(B) Double immunofluorescent labeling shows Mena protein (green) is concentrated at the ends of actin stress fibers (red).

(C) Double immunofluorescent labeling shows Mena protein (green) and anti-phosphotyrosine (red) immunoreactivity.

Bars, 10 μm.

focal adhesions (Figure 4C, see arrowhead). When GST alone was injected, specific labeling was not observed in the cell (data not shown). Therefore, the EVH1 domain likely mediates targeting of Mena to focal adhesions.

To determine if proline-rich ligands recruit Mena to focal adhesions in vivo, we attempted to saturate the N-Mena ligand binding site. A peptide containing the ActA sequence SEPSSFEFPPPPTDEELRLA, which is related to motifs found in zyxin and vinculin, was microinjected into PtK_2 cells. The endogenous Mena protein was depleted from focal contacts in the injected cells (Figure 4D), whereas Mena distribution was not affected by injection of a peptide corresponding to an unrelated portion of ActA, DEWEEEKTEEQPSE (data not shown). Injection of the ActA peptide also depletes VASP focal contacts (Pistor et al., 1995); however, the distribution of vinculin and F-actin stress fibers remained normal (Figures 4E and 4F). Therefore, Mena and VASP do not seem to be required to maintain the integrity of focal contacts or microfilaments in this cell type, at least during the course of this experiment. Together, these data indicate that the N-terminal portion of Mena, which con-

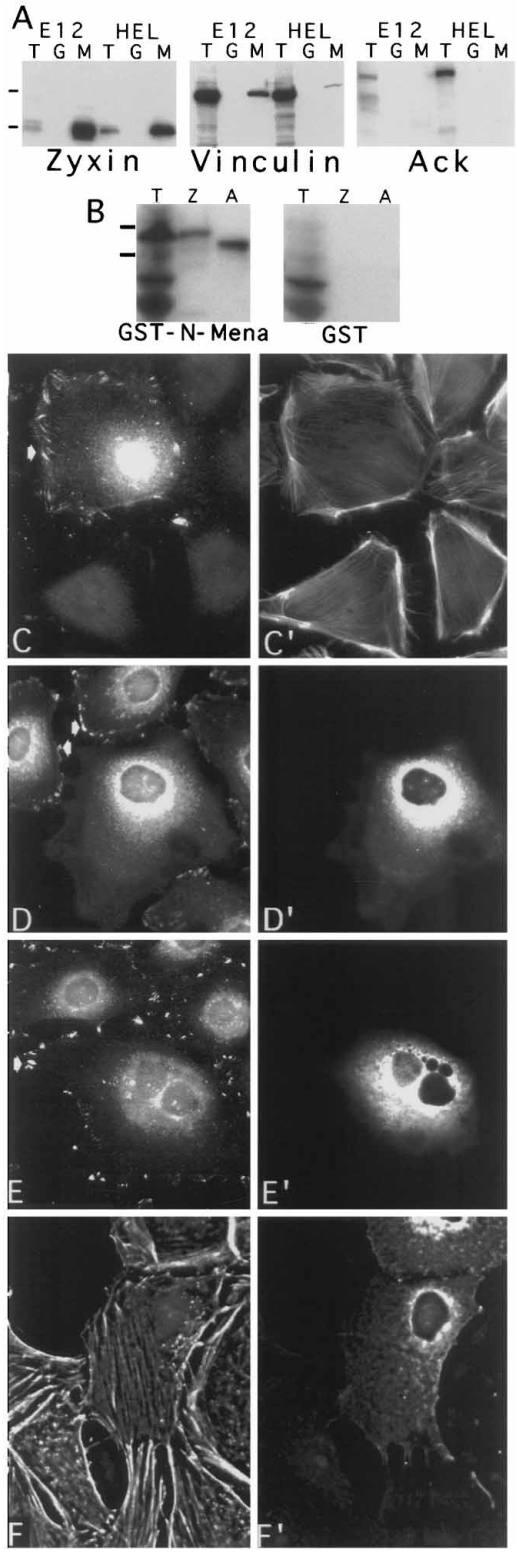

Figure 4. Targeting of Mena to Focal Adhesions Can Be Mediated by Its Amino Terminus and Is Blocked by an ActA-Derived Peptide

(A) RIPA lysates from E12 embryo head extracts or HEL cells were used for a solution binding assay. Twenty μg of total lysates (T), or proteins retained from 500 μg of lysate by GST-sepharose (G), or N-Mena-GST-Sepharose(M) were analyzed by Western blotting with antibodies as indicated. The 116 and 80 kDa markers are indicated by bars.

(B) The GST Mena protein was used for a ligand overlay assay to demonstrate direct binding to zyxin and ActA. Total proteins (50 μg) from human platelets (T), zyxin (~50 ng) purified from porcine platelets (Z) and recombinant Listeria monocytogenes ActA (A) were separated by SDS–PAGE and transferred to nitrocellulose. Sheets were overlaid with GST-N-Mena (5 μg/ml) or an equimolar concentration of GST, and bound proteins were detected with anti-GST antibodies. The purified zyxin and ActA were detected by GST-N-Mena, but not by GST. The major specific signal in the total lysate lane comigrates with purified zyxin. The 97 and 66 kDa markers are indicated by bars.

(C) Anti-GST immunostaining of a cell microinjected with GST-N terminal Mena fusion protein. Phalloidin staining shows the actin stress fibers in the same cells (C′).

(D) Anti-Mena immunofluorescence of PtK_2 cells injected with an ActA peptide, which are marked with coinjected Rhodamine-BSA (D′). In uninjected cells, Mena is concentrated in focal adhesions (see arrowhead).

(E) Anti-vinculin immunofluorescence of cells microinjected with the ActA peptide shows that vinculin remains concentrated in focal adhesions (see arrowhead). Rhodamine-BSA marks the injected cell (E′).

(F) Intact F-actin stress fibers, indicated by phalloidin staining, are present in cells after microinjection of the ActA peptide. Rhodamine-BSA marks the injected cell (F′).

tains the EVH1 domain, can target Mena to focal contacts via protein–protein interactions with molecules containing an ActA-like motif, such as zyxin and vinculin.

Mena Is Recruited to the Surface of Listeria monocytogenes

To determine if Mena is involved in the microfilament assembly required for Listeria motility, we examined infected cells by immunofluorescence and found that Mena was readily detectable on the surface of intracytoplasmic bacteria (Figure 5B). Higher magnification revealed that on motile Listeria, Mena was concentrated on the pole of the bacterium associated with the formation of new actin filaments, at the interface between the bacterium and the actin tail, whereas on nonmotile Listeria, Mena was distributed more uniformly over the bacterial surface (Figures 5C and 5D).

Because the amino terminus of Mena can bind to ActA and an ActA-derived peptide can displace Mena from its normal location within cells, we examined the distribution of the GST-N-Mena fusion protein in Listeria-infected cells. After microinjection of GST-N-Mena into PtK_2 cells followed by infection with Listeria, the exogenous Mena protein was recruited to the bacterial surface (Figures 5E and 5F), whereas microinjected GST protein remained diffusely distributed throughout the cytoplasm of infected cells (data not shown). These results implicate the EVH1 domain in the redistribution of Mena to the bacterial surface.

Mena Is a Ligand for Profilin

Efficient Listeria motility depends on the recruitment of profilin to the bacterial pole adjacent to the newly polymerized actin of the comet tail (Theriot et al., 1994), a process in which VASP has been implicated (reviewed by Pollard [1995]). The profilin-binding site in VASP likely includes the proline-rich sequence $(GP_5)_3G$ since VASP

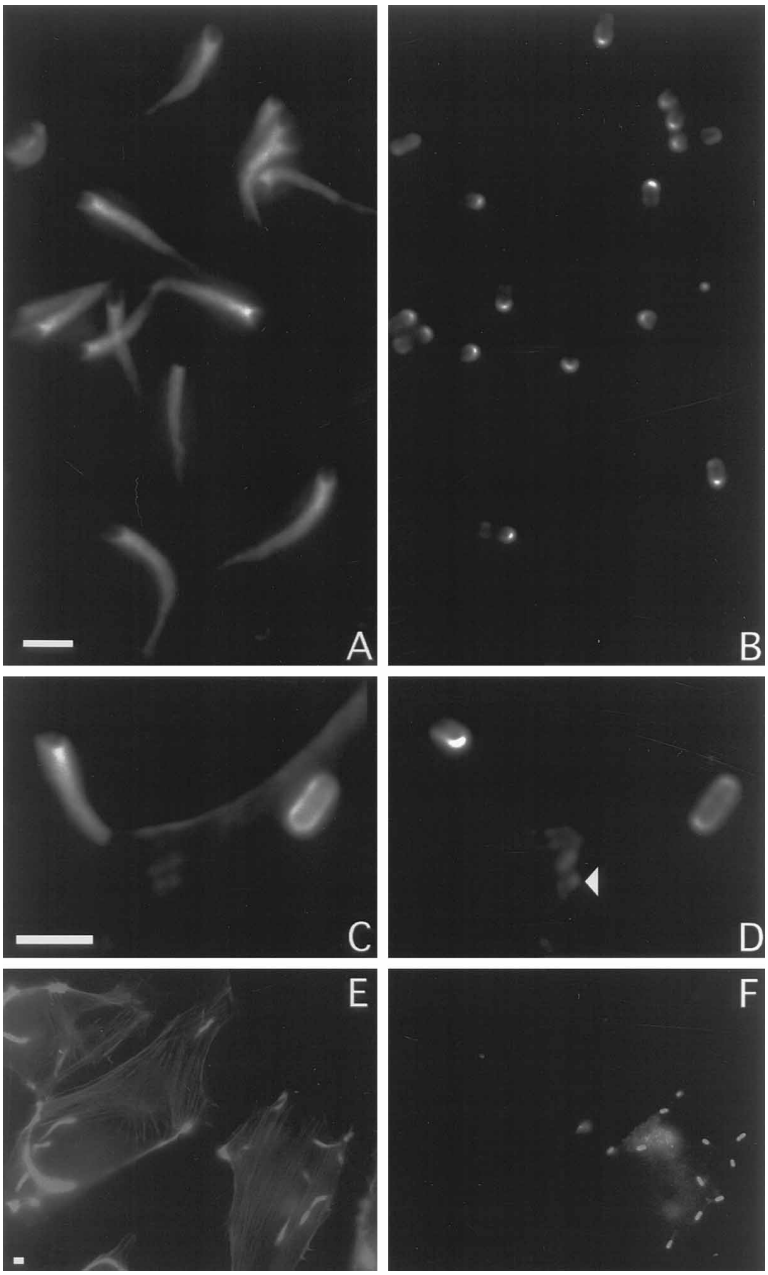

Figure 5. Mena Associates with the Surface of Listeria monocytogenes

Immunofluorescence of PtK_2 cells infected with Listeria shows the distribution of Mena (B) and actin (A). A higher magnification view showing a motile and nonmotile bacteria, indicated by the presence or absence of an actin tail, respectively (C), along with the distribution of Mena (D). An arrowhead in (D) indicates a focal contact labeled with Mena. Cells microinjected with N-Mena fusion protein and infected with Listeria were immunostained using anti-actin (E) and anti-GST antibodies (F). Bar, 2 μm.

dissociates from profilin in the presence of poly-L-proline or $(GP_5)_3G$ (Reinhard et al., 1995a). Since Mena contains related proline-rich motifs, we analyzed the binding of Mena to immobilized profilin. Mena protein translated in vitro was retained on a profilin-sepharose matrix, but not on sepharose alone (Figure 6). Mena binding was reduced 6-fold by preincubation of the profilin matrix with 1 mg/ml of $(GP_5)_3G$ peptide.

We sought to determine whether Mena binds to profilin more efficiently than the $(GP_5)_3G$ peptide. To this end, we reduced the amount of immobilized profilin used in the assay such that approximately half of the Mena protein present in 100 μl of 50 pM ^{35}S-labeled Mena was retained on the matrix. The addition of 500 pM soluble profilin in the assay reduced the amount of Mena retained by the immobilized profilin to ~25% of the input, whereas much higher concentrations (50 μM) of the $(GP_5)_3G$ were required to reduce Mena binding to the same extent. Together, these data suggest that profilin binds Mena much more effectively than the $(GP_5)_3G$ peptide. Further work will be required to determine the binding constant for Mena to profilin.

The Neural-Enriched Mena Isoforms Induce F-Actin Rich Outgrowths in Fibroblasts

The molecular interactions and subcellular distribution of Mena suggest that it may have a role in F-actin formation. We speculated that elevated intracellular concentrations of Mena might stimulate actin nucleation or polymerization. To test this hypothesis, we used a retrovirus to express the different Mena isoforms ectopically in RAT2 cells. Cells were analyzed by immunofluore-

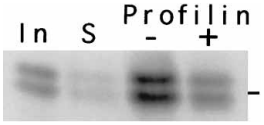

Figure 6. Mena Is a Ligand for Profilin

Ten percent of the protein used in the profilin-binding assay was run as a loading control (In). The amount of Mena retained on sepharose (S), profilin-sepharose in the absence (−) or presence (+) of $(GP_9)_3G$ peptide is shown. Eighty-three percent of the input Mena was retained on the profilin-sepharose as determined by phosphorimager analysis of the gel. Equal binding of the phospho- and dephospho-forms of Mena was observed. In the presence of the competitor peptide, the amount of Mena retained was reduced to 13%. Bar indicates the 80 kDa marker.

sence microscopy to determine the distribution of Mena and F-actin 36 hr after infection with the parental virus (an example is shown in Figure 3B) or viruses expressing the various Mena isoforms. As expected, individual cells within the population expressed varying degrees of the Mena isoforms when analyzed by fluorescence intensity. Similar increases in Mena immunofluorescence intensity across the population were observed with the 80 kDa form or any of the three larger Mena variants. Western blot analysis indicated that, over the whole cell population, the cumulative amount of ectopic Mena$^+$ protein produced was roughly equivalent to the endogenous content of the 80 kDa Mena isoform (Figure 2C). In contrast to the 80 kDa form of Mena, which induced the sporadic formation of small localized clusters of Mena and F-actin (not shown), more dramatic results were observed when any of the three neural-enriched variants of Mena were used (Figure 7). About 25% of the cells had detectable levels of Mena$^+$ immunoreactivity outside focal contacts and often contained concentrated pools of immunoreactivity that overlapped with dense accumulations of F-actin (Figures 7A, 7A′, and 7A′′). Projection of a three-dimensional rendering of the image at a 45° angle indicated that the Mena-actin structures were outgrowths from the cell surface (Figures 7B, 7B′, and 7B′′). An optical section taken at the plane of cell-substratum contact showed a relatively normal distribution of Mena, mainly in focal contacts and at the cell periphery, and F-actin, mainly in typical stress fibers, with only a small amount of the Mena and F-actin deposits (Figures 7C, 7C′, and 7C′′). A section taken 3.8 μm above the substratum contact indicated the Mena-induced projections extend above the top of the nuclei (Figures 7D, 7D′, and 7D′′). Comparison of the Mena and F-actin staining at this level indicated that Mena is distributed at the periphery of the F-actin, potentially at the site of F-actin polymerization and nucleation in these projections (Figure 7D, D′, and D′′, see magnified insets). These data indicate that, when expressed in fibroblasts, the neural-enriched forms of Mena can direct the formation of cell surface outgrowths associated with the recruitment of F-actin.

Discussion

The EVH1 and EVH2 Domains in Mena and Related Proteins

Comparison of the Ena, Mena, Evl, and VASP (the Ena/VASP family) sequences indicated that these proteins share a conserved domains structure. The N-terminal portion of Mena, which contains the EVH1 domain, functions as a modular protein-binding interface that associates with specific proline-rich motifs. Given the high level of conservation of the EVH1 domain at the N-terminus of Ena/VASP family proteins, and the shared ability of Mena and VASP to bind proteins containing the ActA-related proline-rich motif, we propose that the EVH1 domain mediates the association of Ena/VASP family members with proline-rich ligands. The N-Mena binding partners ActA, zyxin, and vinculin all contain the sequence FPPPP, suggesting that this motif may comprise the core of the recognition site in EVH1 ligands. Four different protein modules are known to bind specific proline-rich motifs: SH3 domains (Ren et al., 1993), WW domains, (Chen and Sudol, 1995), profilin (Perelroizen et al., 1994), and now EVH1 domains. While there is no obvious sequence motif shared amongst these domains, they all contain a high concentration of hydrophobic residues, which, in SH3 domains and profilin, are known to make direct contact with prolines (Feng et al., 1994; Perelroizen et al., 1994). Further analyses of EVH1 domains will be needed to define the structural features required for interaction with its ligands.

The N-terminus of Mena is sufficient to target a heterologous protein to sites where Mena is normally concentrated, suggesting that the EVH1 domain of Mena mediates interactions that direct its subcellular distribution. Similar roles in subcellular trafficking have been reported for SH3 domains (Bar Sagi et al., 1993). Displacement of Mena as well as VASP (Pistor et al., 1995) from focal contacts by microinjection of a cognate-ligand peptide suggests that proper localization of both molecules could require binding to proteins containing the FPPPP motif. Two such proteins, zyxin and vinculin, localize to focal adhesions and are among the proteins recovered from lysates on immobilized N-Mena. In addition, N-Mena and VASP (Reinhard et al., 1995b) can bind directly to zyxin in overlay assays. EVH1-mediated associations with zyxin, and potentially vinculin, may link Mena and VASP to other molecules involved in cytoskeletal remodeling and signal transduction.

In solution binding assays, zyxin was more efficiently recovered than vinculin by the N-Mena matrix, suggesting that its affinity for Mena is higher, perhaps due to the presence of 3 FPPPP repeats, or because the binding motif in vinculin is masked by inter- or intramolecular interactions. The Mena-binding motif of vinculin is found in a region thought to form a flexible "hinge" that permits conformational changes required to expose its latent binding activities to F-actin, talin, and other molecules (Johnson and Craig, 1995). These cryptic binding sites in vinculin are unmasked by phosphatidylinositol-4-5-bisphosphate, which disrupts the intramolecular association between the vinculin head domain and the rod-like tail (Gilmore and Burridge, 1996). Perhaps Mena binds to vinculin only in its open conformation. It will be interesting to test this hypothesis and to determine if, when bound to Mena, vinculin can also associate with talin and F-actin.

Another protein, WASP, contains limited identity to the EVH1 domain; juxtaposition of this weak similarity with a proline-rich core suggests that WASP may have some structural features consistent with a functional

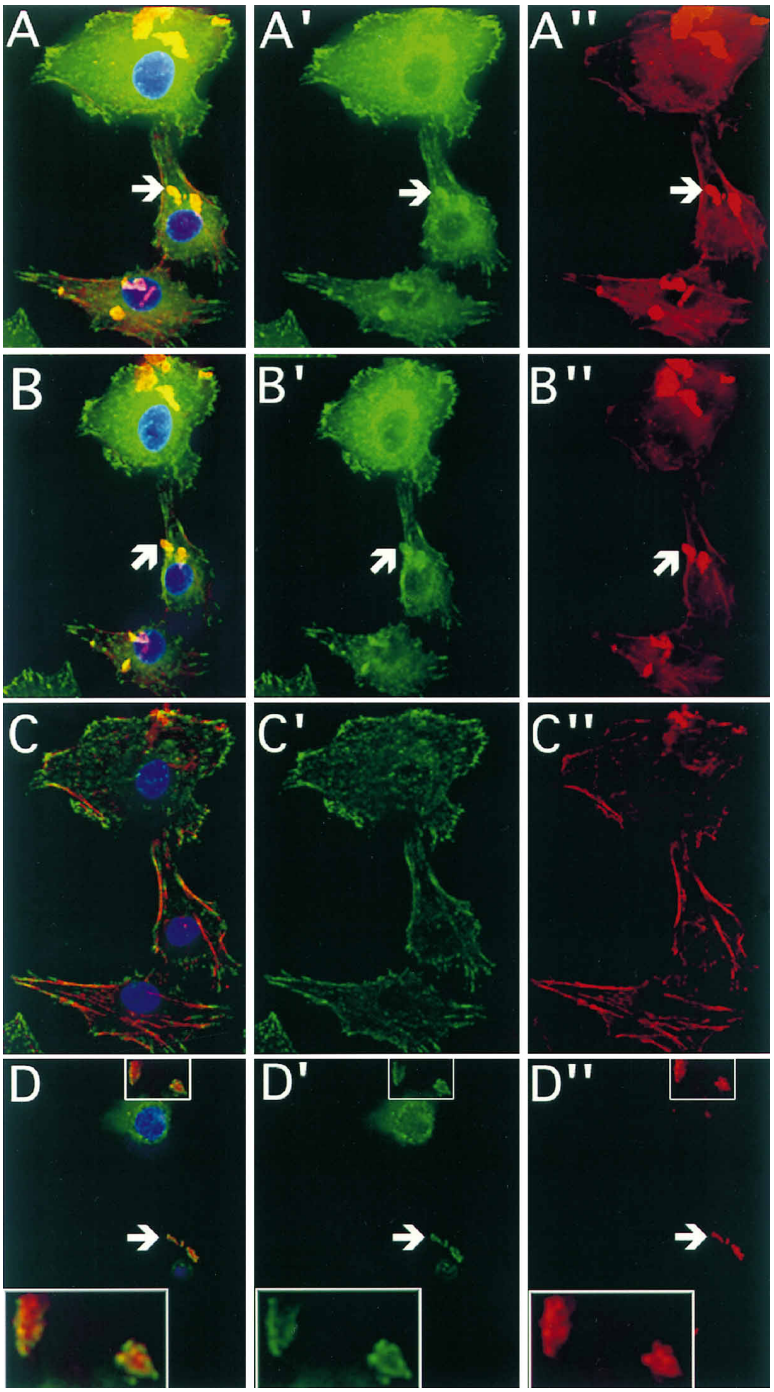

Figure 7. Expression of Neuronal Mena in RAT2 Fibroblasts Induces the Formation of F-Actin Rich Protuberances from the Cell Surface

Immunofluorescence of cells infected with a retrovirus expressing the "+" form of Mena. Mena staining (FITC, green), is shown in (A′), (B′), (C′), and (D′), while actin (Texas red) is shown in (A′′), (B′′), (C′′), and (D′′). The yellow color in the combined images, shown in (A), (B), (C), and (D), indicates overlap between Mena and actin staining. A Z-series of optical sections through the same cells was used to create a 3D projection. This projection is shown rotated at a 45° angle with respect to the plane of the page (B, B′, and B′′). The arrowheads point to the same structure noted in (A). (C), (C′), and (C′′) show an optical section of the same cells at the plane of substratum contact, while an optical section taken 3.8 μM above the level of substrate contact is shown in (D), (D′), and (D′′). The arrowheads in (D) show the same structure noted in (A) and (B). The structures enclosed by the box in (D) are magnified in the inset.

relationship to ENA/VASP family proteins as proposed (Symons et al., 1996). This hypothesis is bolstered by two observations: cellular abnormalities found in WAS patients likely result from defects in the actin-based cytoskeleton (Derry et al., 1994), and ectopic expression of WASP produces clusters of F-actin/WASP aggregates (Symons et al., 1996). The extent to which WASP function overlaps with that of the Ena/VASP family remains to be determined.

As discussed above, the EVH1 domain of VASP may direct its subcellular location by a mechanism similar to that of Mena. However, a previous report suggested that accumulation and concentration of VASP in focal contacts was dependent on its carboxyl terminus. When expressed in BHK21 cells, intact VASP showed the expected distribution of the protein in focal adhesions and along actin stress fibers; however, truncated VASP protein, lacking part of the EVH2 domain (residues 284–380), was not concentrated in focal contacts (Haffner et al., 1995). Differences in the experimental approaches used may account for the apparent discrepancy in the observations. For example, the truncated VASP protein may be improperly folded and incapable of participating in EVH1-mediated interactions. It is also possible that

Ena/VASP proteins are stabilized in focal contacts by their carboxy-terminal EVH2 domain. Perhaps the charged, helical EVH2 domain could promote the formation of stronger multivalent interactions by mediating oligomerization. Consistent with this hypothesis, VASP is thought to form tetramers (Haffner et al., 1995), and the 80 kDa form of Mena coimmunoprecipitates with VASP (F. Gertler, unpublished data), suggesting that homoligomeric and heteromultimeric complexes between different Ena/VASP family proteins may form in vivo. Further experiments will be required to clarify the function of the EVH2 domain.

Mena Function in Listeria Motility

The intracellular propulsion of Listeria depends upon the formation of F-actin-rich comet tails and resembles aspects of the protrusions that occur in spreading and migrating cells (reviewed by Theriot, 1995; Lasa and Cossart, 1996). While controversy exists over the minimal requirements for this motility (Marchand et al., 1995; reviewed by Pollard, 1995), it appears that efficient movement of the bacteria in vivo requires the proline-rich repeats of ActA since microinjection of a peptide comprising an ActA repeat inhibits Listeria motility in cultured cells (Southwick and Purich, 1994). VASP (Chakraborty et al., 1995) and Mena are recruited to Listeria, and bind to ActA, most likely via the proline-rich repeats, thereby implicating these molecules indirectly as factors required for normal Listeria motility.

Efficient Listeria motility may require VASP (reviewed by Pollard, 1995), or Mena, to recruit profilin to the bacterium. The motifs in Mena that mediate binding to ActA and profilin are in separate parts of the protein, potentially allowing simultaneous binding of these two molecules by Mena, thereby serving to recruit profilin (or profilactin complexes) to the surface of Listeria to promote F-actin assembly and bacterial motility.

Profilin (Theriot et al., 1994), VASP (Chakraborty et al., 1995), and in this report, Mena, have been shown to be concentrated at the pole of motile Listeria monocytogenes associated with actin polymerization, while on nonmotile bacteria, Mena and VASP are uniformly distributed. ActA has been observed to be uniformly distributed around both motile and nonmotile Listeria (Niebuhr et al., 1993)—we note that this is a matter of controversy as others have reported a polarized distribution of ActA (Kocks et al., 1993). As proposed for VASP (Chakraborty et al., 1995), the polarized distribution of Mena on the surface of motile Listeria as opposed to ActA might arise from selective modulation of their interaction in vivo, perhaps by posttranslational modification of either protein. The reagents generated in the present study should be useful in the analysis of the polarization process.

Role of Mena in Actin Dynamics

Profilin has been implicated in actin dynamics; for example, it may stimulate F-actin formation by effectively lowering the critical concentration required for monomer addition (Pantaloni and Carlier, 1993; Theriot and Mitchison, 1993). Profilin-actin complexes (profilactin) can bind to polyproline (Perelroizen et al., 1994), and VASP has the capacity to bind to profilin and perhaps profilactin (Reinhard et al., 1995a). Analysis of the aligned sequences revealed that Ena/VASP family proteins contain a short motif similar to sequences that mediate contact between the actin-sequestering molecule thymosin β4 and G-actin (Van Troys et al., 1996). In the Mena/VASP family, the core sequence of this motif, KLKK in thymosin β4, contains one or two arginine residues in place of the two C-terminal lysines (residues noted with an asterisk in Figure 1A). While interpretation of such similarities must be made cautiously, we note that this putative G-actin binding motif is located in the EVH2 domain in close proximity to part of the likely profilin binding region of Mena and VASP. Therefore, it is conceivable that Mena and VASP make direct contacts with both moieties of profilactin complexes. Further analyses will be required to determine whether profilactin is bound by Mena and what effects this complex may have on actin dynamics.

Under normal conditions, Mena could recruit profilin to regions of dynamic actin remodeling via binding to cellular proteins, such as zyxin and vinculin, that contain an ActA-like motif. The involvement of Mena and VASP in promoting efficient actin polymerization is also suggested by the observation that, when targeted to mitochondria, the ability of ActA protein to induce F-Actin recruitment is greatly diminished by deletion of the proline-rich motifs required to recruit VASP, and most likely Mena, to the mitochondrial surface (Pistor et al., 1995).

The ability of exogenous neural Mena isoforms to induce the formation of F-actin-rich outgrowths in fibroblasts is consistent with a role for Mena in the rapid microfilament-based extension of filopodia during axonal growth cone migration, a process that resembles Listeria-induced actin assembly (Forscher et al., 1992). Formation of lammellipodia-like structures can also be induced by introduction of profilactin through microinjection (Cao et al., 1992) or by targeting ActA to the plasma membrane in cultured cells. Expression of a membrane-targeted version of ActA lacking the proline-rich repeats fails to cause such protrusions (Friederich et al., 1995), consistent with the hypothesis that Ena/VASP family proteins may be required for formation of such ActA-induced membrane extensions.

The abnormal F-actin-rich cellular outgrowths induced by Mena$^+$ could result from either the reorganization of existing F-actin, or de novo actin polymerization. The enhanced ability of neural Mena to generate this phenotype as compared to either the 80 kDa form of Mena or VASP (Haffner et al., 1995) arises from inclusion of the proline-rich "+" exon, which could contain additional profilin- or SH3-binding sites. Further analysis will be required to determine the basis for the increased capacity of neural Mena to cause such outgrowths.

What Signals Regulate Mena Function?

Cytoskeletal rearrangement can be elicited by a variety of signal cascades induced by external stimuli such as adhesion through integrins or stimulation with growth factors (Zigmond, 1996). Many of these signals are propagated by kinase cascades that could trigger the observed tyrosine and serine-threonine phosphorylation on Mena. Mena may be a target of cyclic nucleotide

signaling since it contains sequences similar to the known phosphorylation sites for cAMP- and cGMP-dependent kinases in VASP (Butt et al., 1994).

The neural-enriched form of Mena contains phosphotyrosine in vivo. Studies in vitro indicated that c-Src and c-Abl tyrosine kinases could bind Mena via their SH3 domains. Src is concentrated in neuronal growth cones (Bixby and Jhabvala, 1993), and thus is a candidate Mena kinase. By analogy to Drosophila Ena, c-Abl may be linked to Mena. In NIH3T3 cells, c-Abl is largely a nuclear tyrosine kinase (Van Etten et al., 1989); however, we have found a predominantly cytoplasmic distribution of c-Abl in P19 cells and in cells of developing mouse embryos (F. Gertler, unpublished data). A role for c-Abl in actin dynamics is supported by the presence of G- and F-actin binding activities in its C-terminal (McWhirter and Wang, 1991; Van Etten et al., 1994). The potential involvement of Mena in c-Abl and c-Src function is under investigation.

Mena was identified by its similarity to Ena, a molecule implicated in the process of axonogenesis by genetic data. A specialized role for Mena in neural development or function is suggested by three additional lines of evidence. First, concentration of Mena was observed in axonal growth cones, as are two of its binding partners, vinculin (Igarashi et al., 1990) and profilin (Faivre et al., 1993). Second, specific forms of Mena are enriched in the nervous system. Third, unlike VASP or the 80 kDa form of Mena, neural Mena is tyrosine phosphorylated in vivo. Preliminary results of genetic analyses in mice support this hypothesis. Mice homozygous mutant for a targeted disruption of *Mena* exhibit several defects that are, at least superficially, consistent with nervous system defects including: reduced viability after birth, growth retardation, and apparent behavioral abnormalities (F. Gertler and P. Soriano, unpublished data). Detailed analyses of this and other phenotypes at anatomical, and cell biological levels are in progress and should provide further insight into the role of this molecule in the regulation of cell morphology and motility.

Experimental Procedures

Molecular Cloning and Sequence Analysis

Library screening, subcloning, sequencing, and polymerase chain reactions were performed by standard methods. An EcoRI–SphI fragment containing the first 106 codons of Ena (Gertler et al., 1995), or for Evl, the insert of an EST (T08035; obtained from WashU–Merck EST Project IMAGE Consortium, LLNL) was used to screen cDNA libraries made from mouse embryonic stem cells and mouse brain (Stratagene). Sequence analysis was performed using the Genetics Computer Group software package (Devereaux et al., 1984). The BLAST program was used to search the GenBank databases at NCBI.

Fusion Proteins and Antibody Production

Fragments encoding amino acids 6–170 (N-Mena) or 440–537 (C-Mena) were generated by PCR and cloned into pGex2T (Pharmacia). Fusion proteins were prepared and purified on Glutathione-sepharose (Pharmacia), according to the manufacturer's instructions, and used to immunize New Zealand white rabbits. Affinity-purified antisera raised against the peptide LKEELIDAIRQELSKS NTA were produced by QBC.

Biochemistry

Protein extracts from cells or dissected embryos were prepared in ice-cold RIPA buffer (25 mM Tris [pH 7.5]/150 mM NaCl/1% NP40/ 0.5% Deoxycholate/ 0.1% SDS) + 1 mM each PMSF, Aprotinin, and Na_3VO_4. Immunoprecipitations were performed with 1 ml of 1 mg/ml of head lysate using 5 μl of Anti-N-Mena or preimmune sera. Fifty μg of protein were used for Western blotting of total cell lysates. For N-Mena binding assays, 5 μg of N-Mena-GST or GST alone immobilized on glutathione-sepharose were incubated with 1 ml of 1 mg/ml of lysate overnight at 4°C. Samples were washed three times in RIPA and analyzed by Western blotting. Antibody probes used were: anti-peptide Mena, anti-phosphotyrosine mab4G10, or anti-Ack (Santa Cruz) at 1 μg/ml, and anti-zyxin at a 1:100 dilution. Signals were visualized using chemiluminescence (NEN). Ligand overlay assays were conducted as described (Reinhard et al., 1995b).

^{35}S-labeled Mena protein was produced in vitro using the TNT system (Promega) and quantitated by TCA precipitation. Purified protein kinase A and Lambda phosphatase were used according to the manufacturer's (NEB) protocol. Dried gels were fixed and were quantitated using a phosphorimager (Molecular Dynamics). SH3-binding assays were performed as described (Weng et al., 1993).

Purified human platelet profilin (Janmey, 1991) was coupled (at 0.9 mg profilin/ml of matrix) to NHS-activated HiTrap sepharose (Pharmacia). Profilin binding assays were performed as described (Reinhard et al., 1995a), using 20 μl of profilin-sepharose in a 100 μl solution of PBS containing 3% bovine serum albumin followed by three washes PBS before PAGE analysis or scintillation counting. For saturation-binding assays, profilin-sepharose was diluted in sepharose CL4B (Pharmacia) such that the volume of matrix used remained 20 μl.

Cell Culture

RAT2 cells were grown in DMEM (GIBCO) with 10% calf serum. PtK_2 cells (ATCC CCL 56) and 293T cells were grown in MEM (GIBCO) with 10% fetal calf serum, glutamine, and nonessential amino acids. P19 cell culture and differentiation were performed as described (Rudnicki and McBurney, 1987). Retroviruses were constructed by inserting full-length *Mena* cDNAs into the pBABE vector, packaged, and used to infect fibroblasts as described (Morgenstern and Land, 1990).

Microinjection

Purified GST-N-Mena protein or GST was microinjected into the cytoplasm of PtK_2 cells seeded on CELLocate coverslips (Eppendorf) two days earlier. Peptides corresponding to amino acids 293–312 or 41–54 of the ActA sequence were prepared as described (Pistor et al., 1995) and comicroinjected with rhodamine-coupled BSA. The needle concentration of peptide or fusion protein was 2 mM, and ~10% of the total cell volume was injected. Cells were then returned to the incubator for 15 to 30 min before fixation. For subsequent infection with Listeria, cells were allowed to recover for 2 hr.

Immunofluorescence Microscopy

RAT2 cells grown on glass coverslips coated with 5 μg/cm^2 fibronectin (Sigma), and P19 cells grown on ECL growth matrix (UBI) were fixed with 3% or ice cold 4% paraformaldehyde in PBS for 10 min and permeabilized with 0.2% Triton X-100 in PBS. For the detection of microinjected proteins, cells were washed with MES-buffer (0.1 M MES [pH 7.6], 4% PEG 6000 [w/v], 1 mM $MgCl_2$) twice before incubating them with MES-buffer with 0.2% Triton X-100 for 2 min, followed by another MES wash, fixation and staining. Anti-Mena sera were used at 1:400. FITC, Texas red and Cy5 secondary antibody conjugates (Jackson Immunoresearch) were used at 1:100. Phosphotyrosine and neurofilaments were detected using mab4G10 (UBI) and mab 2H3, respectively. Phalloidin, DAPI, and Vectashield mounting media were purchased from Molecular Probes, Sigma, and Vector Labs, respectively. Fluorescence photomicroscopy was conducted on a Zeiss Axiophot, and three-dimensional microscopic images were captured and processed using a Deltavision microscope and software (Applied Precision, Inc.).

Infection of Cultured Cells with Listeria monocytogenes

L. monocytogenes serotype 1/2a EGD were grown in brain-heart infusion broth (Difco) at 37°C with aeration. For infections, bacteria

from an overnight culture were added to PtK_2 cells at a dilution of 1:200. After 1–2 hr, plates were washed with fresh medium containing 25 μg/ml gentamicin. Three hr later, coverslips were washed and processed for immunofluorescence as described above.

Acknowledgments

Correspondence should be addressed to F. B. G. We are deeply indebted to Michael Hoffmann for support during the initial phase of this work. Our thanks go to Mary Beckerle, Trinad Chakraborty, Jonathan Cooper, Frank Ebel, Sal Fuerstenberg, Jeff Hildebrand, Brian Howell, Akira Imamoto, Sheila Thomas, and Ulrich Walter for their support and valuable discussions. We thank Steve Tapscott and Anne Vojtek for critical reading of the manuscrip, Mary Beckerle for anti-zyxin antibodies, Stephan Feller for SH3 fusion constructs, Birgit Gerstel and Josef Wissing for recombinant ActA, Tom Jessell for neurofilament antibody, and Susanne Talay for purified GST and GST-antibodies. We are grateful to Ronald Frank for help with the peptide synthesis, Paul Goodwin for assistance on microscopy, and Brian Howell for P19 cell culture. Use of the image analysis and biotechnology facilities was made possible by core grants to the FHCRC. F. B. G. is a Leukemia Society of America Special Fellow (#3337-95). M. R. is supported by the Deutsche Forschungsgemeinschaft (SFB 176/A21). This work was supported by grants from the National Institutes of Health and Markey Molecular Medicine Center to P. S.

Received May 14, 1996; revised September 6, 1996.

References

Bar Sagi, D., Rotin, D., Batzer, A., Mandiyan, V., and Schlessinger, J. (1993). SH3 domains direct cellular localization of signaling molecules. Cell *74*, 83–91.

Bixby, J.L., and Jhabvala, P. (1993). Tyrosine phosphorylation in early embryonic growth cones. J. Neurosci *13*, 3421–3432.

Butt, E., Abel, K., Krieger, M., Palm, D., Hoppe, V., Hoppe, J., and Walter, U. (1994). cAMP- and cGMP-dependent protein kinase phosphorylation sites of the focal adhesion vasodilator-stimulated phosphoprotein (VASP) in vitro and in intact human platelets. J. Biol. Chem. *269*, 14509–14517.

Cao, L.G., Babcock, G.G., Rubenstein, P.A., and Wang, Y.L. (1992). Effects of profilin and profilactin on actin structure and function in living cells. J. Cell. Biol. *117*, 1023–1029.

Chakraborty, T., Ebel, F., Domann, E., Niebuhr, K., Gerstel, B., Pistor, S., Temm, G.C.J., Jockusch, B.M., Reinhard, M., Walter, U., and Wehland, J. (1995). A focal adhesion factor directly linking intracellularly motile Listeria monocytogenes and Listeria ivanovii to the actin-based cytoskeleton of mammalian cells. EMBO J. *14*, 1314–1321.

Chen, H.I., and Sudol, M. (1995). The WW domain of Yes-associated protein binds a proline-rich ligand that differs from the consensus established for Src homology 3-binding modules. Proc. Natl. Acad. Sci. USA *92*, 7819–7823.

Derry, J.M.J., Ochs, H.J., and Francke, U. (1994). Isolation of a novel gene mutated in Wiskott-Aldrich syndrome. Cell *79*, 635–644.

Devereaux, J., Haeberli, P., and Smithies, O. (1984). A comprehensive set of sequence analysis programs for the VAX. Nucleic Acids Res. *12*, 387–395.

Domann, E., Wehland, J., Rohde, M., Pistor, S., Hartl, M., Goebel, W., Leimeister, W.M., Wuenscher, M., and Chakraborty, T. (1992). A novel bacterial virulence gene in Listeria monocytogenes required for host cell microfilament interaction with homology to the proline-rich region of vinculin. EMBO J. *11*, 1981–1990.

Faivre, S.C., Lena, J.Y., Had, L., Vignes, M., and Lindberg, U. (1993). Location of profilin at presynaptic sites in the cerebellar cortex; implication for the regulation of the actin-polymerization state during axonal elongation and synaptogenesis. Symp. Soc. Exp. Biol. *47*, 317–324.

Feng, S., Chen, J.K., Yu, H., and Schrieber, S.L. (1994). Two binding orientations for peptides to the Src SH3 domain: development of a general model for SH3-ligand interactions. Science *266*, 1241–1247.

Forscher, P., Lin, C.H., and Thompson, C. (1992). Novel form of growth cone motility involving site-directed actin filament assembly. Nature *357*, 515–518.

Friederich, E., Gouin, E., Hellio, R., Kocks, C., Cossart, P., and Louvard, D. (1995). Targeting of Listeria monocytogenes ActA protein to the plasma membrane as a tool to dissect both actin-based cell morphogenesis and ActA function. EMBO J. *14*, 2731–2744.

Geiger, B., Tokuyasu, K.T., Dutton, A.H., and Singer, S.J. (1980). Vinculin, an intracellular protein localized at specialized sites where microfilament bundles terminate at cell membranes. Proc. Natl. Acad. Sci. USA *77*, 4127–4131.

Gertler, F.B., Bennett, R.L., Clark, M.J., and Hoffmann, F.M. (1989). Drosophila abl tyrosine kinase in embryonic CNS axons: a role in axonogenesis is revealed through dosage-sensitive interactions with *disabled*. Cell *58*, 103–113.

Gertler, F.B., Doctor, J.S., and Hoffmann, F.M. (1990). Genetic suppression of mutations in the Drosophila abl proto oncogene homolog. Science *248*, 857–860.

Gertler, F.B., Hill, K.K., Clark, M.J., and Hoffmann, F.M. (1993). Dosage-sensitive modifiers of Drosophila abl tyrosine kinase function: prospero, a regulator of axonal outgrowth, and disabled, a novel tyrosine kinase substrate. Genes Dev. *7*, 441–453.

Gertler, F.B., Comer, A.R., Juang, J.L., Ahern, S.M., Clark, M.J., Liebl, E.C., and Hoffmann, F.M. (1995). enabled, a dosage-sensitive suppressor of mutations in the Drosophila Abl tyrosine kinase, encodes an Abl substrate with SH3 domain-binding properties. Genes Dev. *9*, 521–533.

Gilmore, A.P., and Burridge, K. (1996). Regulation of vinculin binding to talin and actin by phosphatidylinositol-4-5-bisphosphate. Nature *381*, 531–535.

Haffner, C., Jarchau, T., Reinhard, M., Hoppe, J., Lohmann, S.M., and Walter, U. (1995). Molecular cloning, structural analysis and functional expression of the proline-rich focal adhesion and microfilament-associated protein VASP. EMBO J. *14*, 19–27.

Halbrügge, M., and Walter, U. (1989). Purification of a vasodilator-regulated phosphoprotein from human platelets. Eur. J. Biochem. *185*, 41–50.

Henkemeyer, M., West, S.R., Gertler, F.B., and Hoffmann, F.M. (1990). A novel tyrosine kinase-independent function of Drosophila abl correlates with proper subcellular localization. Cell *63*, 949–960.

Igarashi, M., Saito, S., and Komiya, Y. (1990). Vinculin is one of the major endogenous substrates for intrinsic tyrosine kinases in neuronal growth cones isolated from fetal rat brain. Eur. J. Biochem. *193*, 551–558.

Janmey, P.A. (1991). Polyproline affinity method for purification of platelet profilin and modification with pyrene-maleimide. Methods Enzymol. *196*, 92–99.

Johnson, R.P., and Craig, S.W. (1995). F-actin binding site masked by the intramolecular association of vinculin head and tail domains. Nature *373*, 261–264.

Kocks, C., Hellio, R., Gounon, P., Ohayon, H., and Cossart, P. (1993). Polarized distribution of Listeria monocytogenes surface protein ActA at the site of directional actin assembly. J. Cell Sci. *105*, 699–710.

Lasa, I., and Cossart, P. (1996). Actin-based bacterial motility: towards a definition of the minimal requirements. Trends Cell Biol. *6*, 109–114.

Lauffenburger, D.A., and Horwitz, A.F. (1996). Cell migration: a physically integrated molecular process. Cell *84*, 359–369.

Maher, P.A., Pasquale, E.B., Wang, J.Y., and Singer, S.J. (1985). Phosphotyrosine-containing proteins are concentrated in focal adhesions and intercellular junctions in normal cells. Proc. Natl. Acad. Sci. USA *82*, 6576–6580.

Manser, E., Leung, T., Salihuddin, H., Tan, L., and Lim, L. (1993). A non-receptor tyrosine kinase that inhibits the GTPase activity of p21cdc42. Nature *363*, 364–367.

Marchand, J.B., Moreau, P., Paoletti, A., Cossart, P., Carlier, M.F.,

and Pantaloni, D. (1995). Actin-based movement of Listeria monocytogenes: actin assembly results from the local maintenance of uncapped filament barbed ends at the bacterium surface. J. Cell Biol. *130*, 331–343.

McWhirter, J.R., and Wang, J. (1991). Activation of tyrosine kinase and microfilament-binding functions of c-abl by bcr sequences in bcr/abl fusion proteins. Mol. Cell. Biol. *11*, 1553–1565.

Mitchison, T.J., and Cramer, L.P. (1996). Actin-based cell motility and cell locomotion. Cell *84*, 371–379.

Morgenstern, J.P., and Land, H. (1990). Advanced mammalian gene transfer: high titre retroviral vectors with multiple drug selection markers and a complementary helper-free packaging cell line. Nucleic Acids Res. *18*, 3587–3596.

Niebuhr, K., Chakraborty, T., Rohde, M., Gazlig, T., Jansen, B., Kollner, P., and Wehland, J. (1993). Localization of the ActA polypeptide of Listeria monocytogenes in infected tissue culture cell lines: ActA is not associated with actin "comets." Infect. Immun. *61*, 2793–2802.

Pantaloni, D., and Carlier, M.F. (1993). How profilin promotes actin filament assembly in the presence of thymosin β4. Cell *75*, 835–838.

Perelroizen, I., Marchand, J.-B., Blanghoin, L., Didry, D., and Carlier, M.-F. (1994). Interaction of profilin with G-actin and poly-L-proline. Biochem. *33*, 8472–8478.

Pistor, S., Chakraborty, T., Walter, U., and Wehland, J. (1995). The bacterial actin nucleator protein ActA of Listeria monocytogenes contains multiple binding sites for host microfilament proteins. Curr. Biol. *5*, 517–525.

Pollard, T.D. (1995). Actin cytoskeleton. Missing link for intracellular bacterial motility? Curr. Biol. *5*, 837–840.

Reinhard, M., Halbrügge, M., Scheer, U., Wiegand, C., Jockusch, B.M., and Walter, U. (1992). The 46/50 kDa phosphoprotein VASP purified from human platelets is a novel protein associated with actin filaments and focal contacts. EMBO J. *11*, 2063–2070.

Reinhard, M., Giehl, K., Abel, K., Haffner, C., Jarchau, T., Hoppe, V., Jockusch, B.M., and Walter, U. (1995a). The proline-rich focal adhesion and microfilament protein VASP is a ligand for profilins. EMBO J. *14*, 1583–1589.

Reinhard, M., Jouvenal, K., Tripier, D., and Walter, U. (1995b). Identification, purification, and characterization of a zyxin-related protein that binds the focal adhesion and microfilament protein VASP (vasodilator-stimulated phosphoprotein). Proc. Natl. Acad. Sci. USA *92*, 7956–7960.

Ren, R., Mayer, B.J., Cicchetti, P., and Baltimore, D. (1993). Identification of a ten-amino acid proline-rich SH3 binding site. Science *259*, 1157–1161.

Rudnicki, M.A., and McBurney, M.W., (1987). Cell culture methods and induction of differentiation of embryonal carcinoma cell lines. In Teratocarcinomas and Embryonic Stem Cells: A Practical Approach. E. Robertson, ed. (Oxford: IRL Press), pp. 19–47.

Sadler, I., Crawford, A.W., Michelsen, J.W., and Beckerle, M.C. (1992). Zyxin and cCRP: two interactive LIM domain proteins associated with the cytoskeleton. J. Cell. Biol. *119*, 1573–1587.

Southwick, F.S., and Purich, D.L. (1994). Arrest of Listeria movement in host cells by a bacterial ActA analogue: implications for actin-based motility. Proc. Natl. Acad. Sci. USA *91*, 5168–5172.

Symons, M., Derry, J.M.J., Karlok, F., Jiang, S., Lemahieu, V., McCormick, F., Francke, U., and Abo, A. (1996). Wiskott-Aldrich syndrome protein, a novel effector for the GTPase CDC42Hs, is implicated in actin polymerization. Cell *84*, 723–734.

Theriot, J.A. (1995). The cell biology of infection by intracellular bacterial pathogens. Annu. Rev. Cell Dev. Biol. *11*, 213–239.

Theriot, J.A., and Mitchison, T.J. (1993). The three faces of profilin. Cell *75*, 835–838.

Theriot, J.A., Rosenblatt, J., Portnoy, D.A., Goldschmidt, C.P.J., and Mitchison, T.J. (1994). Involvement of profilin in the actin-based motility of L. monocytogenes in cells and in cell-free extracts. Cell *76*, 505–517.

Van Etten, R.A., Jackson, P., and Baltimore, D. (1989). The mouse type IV c-abl gene product is a nuclear protein, and activation of transforming ability is associated with cytoplasmic localization. Cell *58*, 669–678.

Van Etten, R.A., Jackson, P.K., Baltimore, D., Sanders, M.C., Matsudaira, P.T., and Janmey, P.A. (1994). The COOH terminus of the c-Abl tyrosine kinase contains distinct F. and G. actin binding domains with bundling activity. J. Cell Biol. *124*, 325–340.

Van Troys, M., Dewitte, D., Goethals, M., Carlier, M.F., Vandekerckhove, J., and Ampe, C. (1996). The actin binding site of thymosin β4 mapped by mutational analysis. EMBO J. *15*, 201–210.

Weng, Z., Taylor, J.A., Turner, C.E., Brugge, J.S., and Seidel, D.C. (1993). Detection of Src homology 3-binding proteins, including paxillin, in normal and v-Src-transformed Balb/c 3T3 cells. J. Biol. Chem. *268*, 14956–14963.

Zigmond, S.H. (1996). Signal transduction and actin filament organization. Curr. Opin. Cell Biol. *8*, 66–73.

GenBank Accession Numbers

The GenBank accession numbers for the Evl, Mena, Mena^{+}, Mena^{++}, and Mena^{+++} sequences are U72519, U72520, U72521, U72522, and U72523, respectively.